IEEE Access
Multidisciplinary ⋮ Rapid Review ⋮ Open Access Journal

Received 20 September 2022, accepted 7 October 2022, date of publication 13 October 2022, date of current version 20 October 2022.

Digital Object Identifier 10.1109/ACCESS.2022.3214313

RESEARCH ARTICLE

Design of a Compact Novel Stub Loaded Pentaband Bandpass Filter for Next Generation Wireless RF Front Ends

BILAL MUSHTAQ, SOHAIL KHALID, (Member, IEEE), AND MUHAMMAD ABDUL REHMAN
Department of Electrical Engineering, Riphah International University, Islamabad 45210, Pakistan

Corresponding author: Bilal Mushtaq (bilalmushtaq88@outlook.com)

ABSTRACT This paper presents a compact novel pentaband bandpass filter using a dual path stub loaded step impedance resonator (SLSIR). The proposed topology consists of a dual path λ/4 and 2λ/3 long uniform impedance resonator centered separated by 2λ/3 open and λ/12 short circuit stubs respectively. The superposition of signals from the two transmission routes results in a fifth-order pentaband bandpass response with six finite frequency transmission zeroes and out-of-band rejection of 11dB from 12 GHz up to 20 GHz. The filter produces five frequency bands at 1.06 GHz, 3.24 GHz, 5.36 GHz, 8.55 GHz and 10.78 GHz with fractional bandwidth (FBW) of 25.59%, 22.22%, 19.48%, 16.03% and 17.17% respectively. The proposed design is fabricated on a high-frequency substrate with a physical size of ($0.23\lambda_g \times 0.14\ \lambda_g$). The new pentaband bandpass filter has a simple and compact design with good electrical performance. A fair match can be found between the simulated and experimental results.

INDEX TERMS Bandpass filter, step impedance resonator, microwave filters.

I. INTRODUCTION

Band Pass Filter (BPF) is an integral component of the RF and microwave framework system to obviate signal interference, remove unwanted signals, and maintain low insertion loss within the passbands. Rapid technological growth in wireless communication systems leads to increasing demand for multiband bandpass filters. One of the major issues in designing a multiband communications system is to acquire a small size. For that reason, extensive research has been done in the miniaturization of such systems and one limitation is the system itself. Instead of incorporating multiple filters of a single band to achieve the desired response, it would be more appropriate to have a specific filter that will provide multiband response. Due to its multi-functionality and size reduction features, multiband multi-mode bandpass filters have become a critical part of modern-day communication systems. Numerous practices [1], [2], [3], [4], [5], [6], [7], [8], [9], [10], [11], [12], [13], [14], [15], [16] have been used in the designing of multiband bandpass filters. A dual bandpass topology based on a coupled three-section stepped impedance resonator (SIR) was introduced [1]. However the design has a lower out of band rejection and large circuit size. Another dual-band bandpass filter (BPF) is proposed in [2]. It has a wide stopband and a small and wide passband. For narrow and wide passband response, a step impedance ring loaded resonator (SIRLR) is used; for a broader stopband response, a rectangular stub loaded resonator (RSLR) is used. Resonance modes due to SIRLR are used to obtain dual passbands with an insertion loss of less than 1.5 dB for both bands. However, the design did not provide adequate suppression of interference in the stopband. In [3], the Tri-band bandpass filter topology is introduced, which sandwiches a single band filter between two double band sub-filters. Although the suggested filter exhibits acceptable electrical performance, the addition of a separate filter increases the circuit size. Reference [4] presents a tri-band bandpass filter with symmetrical open stub loaded SIR method. Tri stub-loaded SIR is used to generate a triple band, the centre frequency of which is independently adjusted. The design, on the other hand, has a low out-of-band rejection. A multilayer design that corresponds to a triple-band bandpass filter response

The associate editor coordinating the review of this manuscript and approving it for publication was Yiming Huo.

This work is licensed under a Creative Commons Attribution-NonCommercial-NoDerivatives 4.0 License.
For more information, see https://creativecommons.org/licenses/by-nc-nd/4.0/

is presented in [5]. The proposed design topology did not achieve minimal insertion loss, compact size, or ease of design, as the multi-layered structural method made this fabrication more complex. The SIR-based approach to designing a triple-band bandpass filter is presented in [6]. There is no transmission zero in this design. Also, the size of the predicted filter is too large that will limit its use. Moreover, [7] created a three-passband bandpass filter with a tri-section SIR. While the performance of the design remains same, the size is reduced by half compared to [6]. A quad-band bandpass filter with a stub-loaded resonator is presented in [8]. The design incorporates four passbands with three transmission zeros to four transmission poles. While the topology resulted in a more compact and simple design, still it did not result in improved out-of-band rejection. Cheng et al. [9] proposed a quad-band bandpass filter on a ceramic substrate by combining four primary microstrip topologies. A quad band bandpass filter presented in [10] used a quad mode resonator. The design is straightforward, compact, and easy to build. In general, quad-band bandpass filters can be designed using three different ways. To begin, a quad-band resonator is used [8], [10]. The second method employs a dual bandpass filter and inserts transmission zero within the passband, effectively splitting the dual passband in half to obtain a quad-band response [11]. Thirdly, the quad-band response can be obtained by connecting two dual bandpass filters in parallel [12], [13]. A pentaband bandpass filter with an asymmetric interdigital couple line is presented in [14]. The electrical performance of the design is satisfactory. The design complexity is substantial and the proposed passbands are at lower frequencies. In [15], a pentaband bandpass filter based on multilayer technology is presented. Despite its good electrical performance, the circuit size is relatively large and the passbands are at lower frequencies. Circuit fabrication is also complicated owing to the multilayer substrate.

However, the multi-band multi-mode bandpass filters stated above require numerous layers of fabrication and a variety of resonators, limiting their application breadth, increasing the cost and complexity of the design and fabrication process.

A novel compact pentaband bandpass filter based on a dual path stub loaded step impedance resonator (SLSIR) is presented in this paper. The design consists of a dual-path having two symmetrical transmission lines and a short-circuit stub in path-1, and SIR sections with an open-circuit stub in path-2. Collectively, both paths generate ten transmission poles (TPz) for passband visualisation and six in-band transmission zeros (TZs) to improve selectivity. The proposed design achieved improved electrical performance and ease of fabrication. The simulated and measured results are a fair match.

II. DESIGN PROCEDURE

Figure 1 shows the design topology of the proposed pentaband bandpass filter. The topology consists of two propagation paths. Path 1 consists of two transmission lines with characteristic impedance Z_1 and θ_1 electrical length

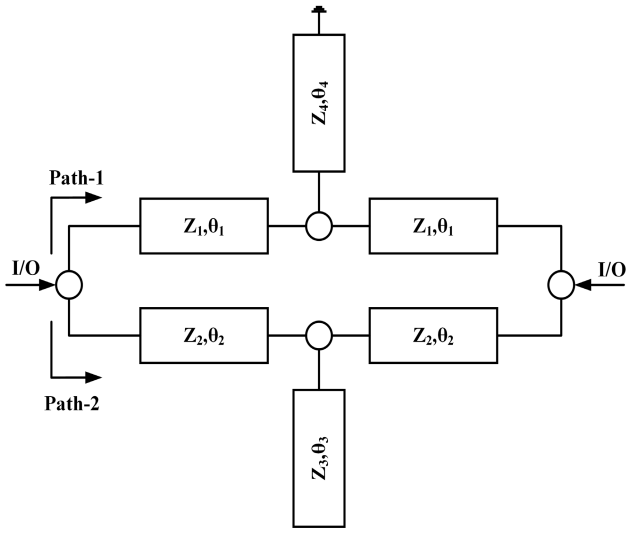

FIGURE 1. Topology layout model of designed Pentaband BPF.

connected by a tapped short circuit stub with characteristic impedance Z_4 and θ_4 electrical length. While path 2 connects two transmission lines with a characteristic impedance of Z_2 and θ_2 electrical length, an open-circuit stub is crammed between them with a characteristic impedance of Z_3 and θ_3 electrical length. In this configuration, the proposed topology gives a pentaband multi-mode passband response.

The total ABCD transfer matrix of path-1 consisting of transmission line and short circuit stub is.

$$T_{Path-1} = T_{UIR1} \times T_{SCS} \times T_{UIR1} \tag{1}$$

For the simplification, $\theta_1 = \theta_2 = \theta_3 = \theta_4 = \theta$ and $Z_1 = Z_2 = Z_3 = Z_4 = Z$ are considered. As Both paths are parallel to each other so considering admittance (Y-matrix) will be more provident instead of impedance matrix. The Y-matrix of path-1 will be

$$Y^{i=path} = \begin{bmatrix} Y_{11} & Y_{12} \\ Y_{21} & Y_{22} \end{bmatrix} \tag{2}$$

where,

$$Y^1_{11} = Y^1_{22} = \frac{-1/3j(3cos^2\theta - 1)}{Zsin\theta cos\theta} \tag{3}$$

$$Y^1_{12} = Y^1_{21} = \frac{-1/3j}{Zsin\theta cos\theta} \tag{4}$$

where equations 3 and 4 represent the admittance matrix coefficient of path-1. The transfer matrix of path-2 is.

$$T_{Path-2} = T_{UIR2} \times T_{OCS} \times T_{UIR2} \tag{5}$$

$$Y^2_{11} = Y^2_{22} = \frac{-jcos\theta(3cos^2\theta - 2)}{Zsin\theta(3cos^2\theta - 1)} \tag{6}$$

$$Y^2_{12} = Y^2_{21} = \frac{jcos\theta)}{Zsin\theta(3cos^2\theta - 1)} \tag{7}$$

$$Y_{total} = Y^1 + Y^2 \tag{8}$$

After the ABCD and Y-parameter conversion of both paths, the overall Y-matrix of design is calculated using equation 8

and the S-parameter of the proposed filter design can be written as [21].

$$S_{12} = \frac{-2Y_{21}Y_O}{(Y_O + Y_{11})^2 - Y_{21}^2} \tag{9}$$

where $Y_O = 1/Z_O$, $Z_O = 50\Omega$ is the reference impedance of the system and $Y_{11} = (D_1/B_1) + (D_2/B_2)$ and $Y_{21} = (-1/B_1) + (-1/B_2)$. The relationship between the transmission coefficient and filtering function [21] is used to find the overall filtering function.

$$|S_{12}(\theta)|^2 = \frac{1}{1 + \epsilon^2 F_N^2(\theta)} \tag{10}$$

The N^{th} order filtering function is denoted by $F_N(\theta)$. The proposed filter design's resulting filtering function is of 5^{th} order (N = 5). Filtering function of proposed 5^{th} order BPF design is given in the equation 11.

$$F_N^2(\theta) = \frac{1}{2Z\omega}(\alpha cos^{10}\theta + \beta cos^8\theta + \gamma cos^6\theta + \delta cos^4\theta + \rho cos^2\theta + \tau)^{1/2} \tag{11}$$

Here filter coefficient is $\omega, \alpha, \beta, \gamma, \delta, \rho$ and τ are calculated as.

$$\omega = (36cos^6\theta - 48cos^4\theta + 13cos^2\theta - 1)^{1/2} \tag{12}$$
$$\alpha = -81(Z-2)^2(Z+2)^2 \tag{13}$$
$$\beta = 216Z^4 - 1512Z^2 + 2592 \tag{14}$$
$$\gamma = -198Z^4 - 1008Z^2 - 1584 \tag{15}$$
$$\delta = 72Z^4 - 120Z^2 + 288 \tag{16}$$
$$\rho = -9Z^4 - 28Z^2 - 16 \tag{17}$$
$$\tau = 4Z^2 \tag{18}$$

Equation 11 illustrates the topology filtering function seen in Figure 1. The filtering function can be transformed to a type 1 chebyshev polynomial for the extraction of electrical parameter values. By selecting proper characteristic impedance values, as shown in equation 11, six transmission poles can be generated. The filtering coefficient, defined by equations 12 - 18, is used to calculate the position of transmission poles and ripple peaks. The total electrical length of path-1 and path-2 is undergone through constructive interference, which leads to the multi-passband response at higher frequencies. The filtering function above also depicts that the filter is of 5^{th} order.

It is observed that by altering the electrical length of the uniform impedance resonator in path 2, the position of transmission zeros can be controlled. As shown in figure 2(a), For $\theta_1 = 80°$, it is noted that by varying the θ_1 to lower side, value the transmission zero shift toward higher frequencies. Also, by varying θ_1 to higher angular value, the transmission zeros shift toward lower frequencies as shown in figure 2(b).

Transmission zeros are created among each passband using the multi-paths propagation setup to enhance passband selectivity and produce better separation. The open-circuit stub connected in path-2 generates one additional passband along

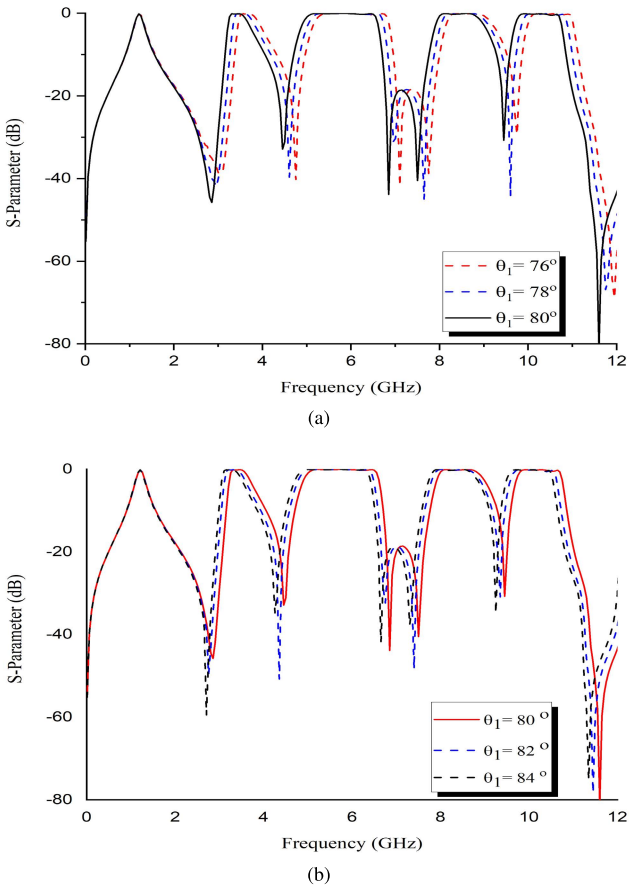

FIGURE 2. Frequency response vs θ_1 (a) $< \theta_1$, (b) $> \theta_1$.

with the control over the 2^{nd}, 3^{rd}, and 5^{th} passband. While grounding the stub in path-1 gives a passband response.

Short circuit stubs induce band to band separation. It is noted that by regulating the physical length of short circuit stub fractional bandwidth of 1^{st},2^{nd}, and 4^{th} passband can be adjusted as illustrated in figure 3. When the physical length is increased, the fractional bandwidth of the 2^{nd} and 4^{th} passband decreases, while the fractional bandwidth of the 1^{st} passband increases. It is observed that adjusting the physical length of a short circuit stub does not influence the 3^{rd} or 5^{th} passband.

The electrical length of the transmission line topology (Figure 1) is very high, restricting the desired performance and compact design from being obtained. To realize the bandpass filter, a SLSIR is used in path-2. Each transmission line of SIR has distinct impedance values corresponding to varying physical widths. The step impedance resonator [22] also provides additional transmission zeros between passbands in addition to enhancing the compactness of the structure by regulating the electrical length to the appropriate value.

A step impedance resonator is used at two points in path-2, as indicated in figure 5. Without SIR, the suggested topology yields three passbands while keeping all physical characteristics constant. The use of SIR in design results in the generation of five passbands.

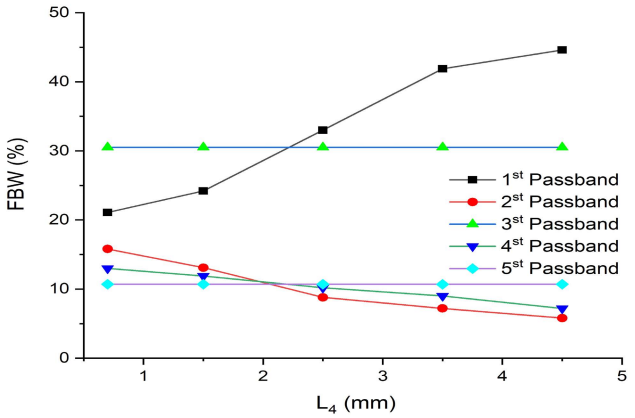

FIGURE 3. FBW vs L_4.

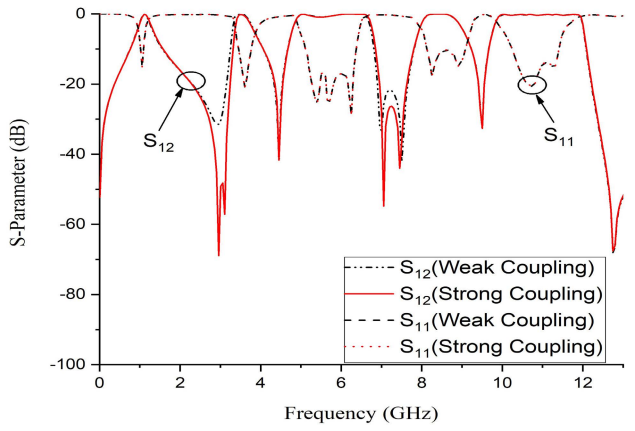

FIGURE 4. Frequency response with coupling.

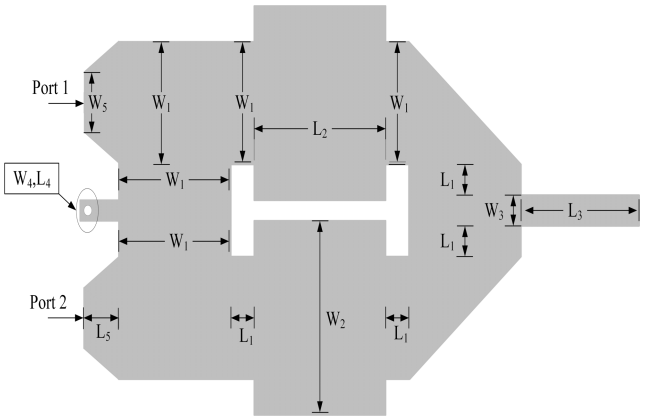

FIGURE 5. Block diagram of compact pentaband BPF.

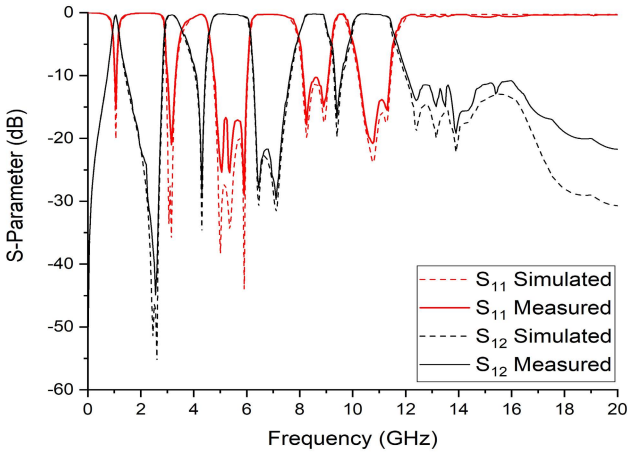

FIGURE 6. S-parameter response of simulated and fabricated design.

Additionally, the use of SIR in the design creates a coupling effect. The width W_2 of the thick region determines the coupling strength. As a result of the coupling effect, there are more transmission zeros, which increases selectivity. The rejection level between the 1^{st}-2^{nd} and 3^{rd}-4^{th} passbands has increased from 31.18 dB to 48.67 dB and 21.71 dB to 26.26 dB, respectively, as shown in 4.

III. RESULTS

Microstrip transmission lines are used to implement the compact design of the proposed topology. The proposed pentaband BPF design is intended for use with Roger Duriod RT/5880 substrate. The substrate has a relative dielectric constant ($\epsilon_r = 2.2$), dielectric loss tangent (tan $\delta = 0.0009$), and thickness ($H = 0.787mm$).

Figure 5 depicts the configuration of the proposed filter. The physical dimensions are L_i and W_i, where L_i is the microstrip line's length and W_i is the width. Using line calculator, the physical parameters are calculated as $W_1 = 7.36$, $W_2 = 12.03$, $W_3 = 3.23$, $W_4 = 0.7$, $L_1 = 1.92$, $L_2 = 9.42$, $L_3 = 9.42$, $L_4 = 1$ and, $R_{via-hole} = 0.2$ respectively (unit is mm).

The final integration of simulated and Measured results is shown in figure 6 having five passbands with fractional bandwidth (FBW) of 25.59%, 22.22%, 19.48%, 16.03%, and 17.17% respectively. The maximum insertion loss (S_{21}) within passband 0.35 dB, 0.37 dB, 0.17 dB, 0.19 dB, 0.20 dB and while the minimum return loss (S_{11}) in all passbands is less than 11.24 dB respectively. The slight variance between simulated and measured results may be attributed to fabrication tolerance, material variance, and connectors losses. Such discrepancies may be controlled by post-fabrication fine-tuning. It is worth noting that no post-fabrication tweaking was performed.

The isolation among the passbands is more than 15 dB. Besides, the fabricated pentaband bandpass filter also has a rejection of more than 11.3 dB from 12 GHz to 20 GHz at the upper stopband. Figure 7, depicts the electric field spectrum at various resonant frequencies, (a) 3.40 GHz, (b) 10.7 GHz, (c) 0.3 GHz, and (d) 2.02 GHz for the proposed filter design. As the maximum field is contained, it demonstrates that for five resonant frequencies, nearly the entire circuit contributes. Figure 8 illustrate the anticipated group delay in five passbands is no more than 1.25ns, with the first passband (1.25ns),

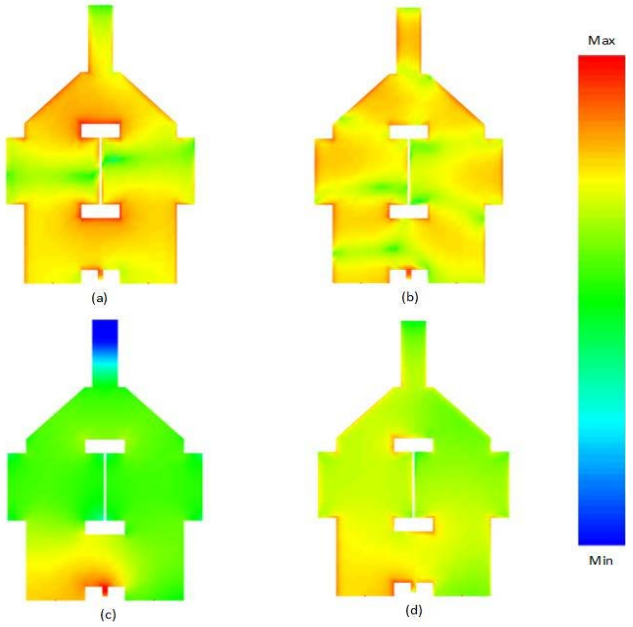

FIGURE 7. Electric field spectrum of proposed PBBPF.

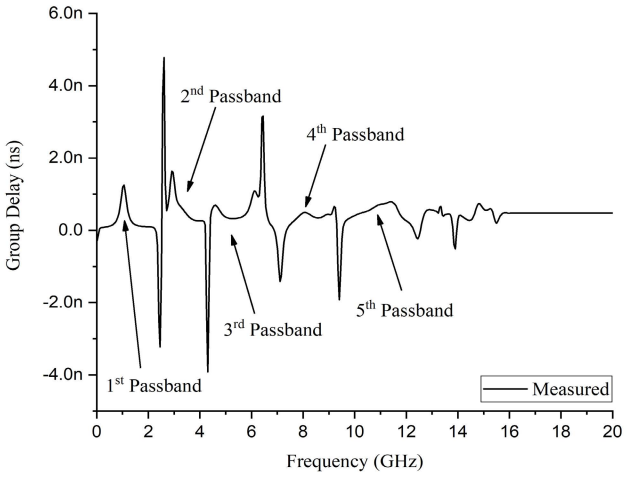

FIGURE 8. Group delay.

the second passband (0.65*ns*), the third passband (0.38*ns*), the fourth passband (0.34*ns*), and the fifth passband (0.68*ns*) respectively.

The benefit of the proposed PBBPF over previously developed bandpass filters is illustrated in Table1.

It is observed that the proposed pentaband bandpass filter has a higher number of TP's and TZ's, resulting in better selectivity at higher frequencies. In addition to being compact, wide out of band rejection and having a good fractional bandwidth, the proposed PBBPF structure provides a combination of narrow, medium, and wideband frequency responses at the same time. The proposed design is simple and easy to fabricate. The fabricated pentaband bandpass filter is shown in figure 9.

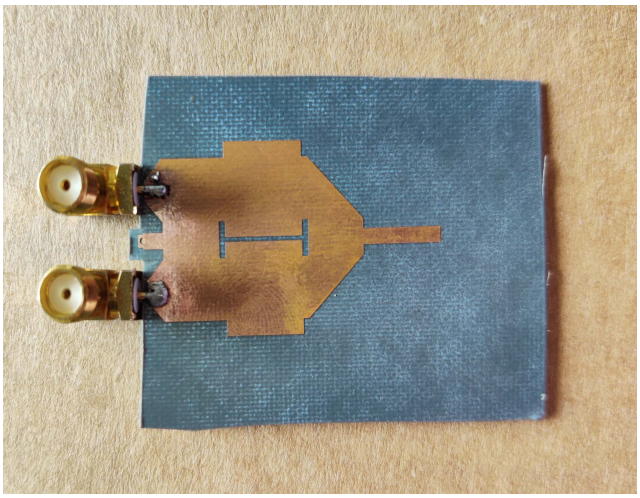

FIGURE 9. Fabricated prototype.

TABLE 1. Comparison of the fabricated prototypes.

Ref.	PB	CF (GHz)	IL (dB)	RL (dB)	FBW (%age)	Circuit size ($\lambda_g \times \lambda_g$)
[1]	2	0.61/1.36	0.45/0.75	>10	32.3/10.5	2.44×0.48
[4]	3	0.9 /2.45/5.5	0.64 /0.68/1.4	>9.2	23 /10/17	0.13×0.16
[8]	4	1.5/2.5 /3.6/4.6	1.98/1.74 /3.58/3.4	>12	5.5/12 /11/4.3	0.3×0.3
[10]	4	1.9/2.8 /4.3/5.2	2.3/3.6 /3.5/3.4	>10	5.3/3.4 /3.5/3	0.19×0.13
[11]	4	1.74/2.09 /2.75/ 3.14	1.4/1.7 /2.1/2.6	>11	6.89/3.82 /2.25/1.59	0.19×0.20
[12]	4	2.4/3.5 /5.2/6.8	0.5/1.3 /1.3/1	>10	6.4/9.4 /3.8/4.9	0.3×0.3
[13]	4	1.55/2.79 /3.29/4.47	4.42/2.63 /3.03/5.11	>11	3.1/3.22 /2.79/2.23	0.26×0.08
[14]	5	1.8/ /2.4/3.5 /4.9/5.8	1.1 /0.95/1.35 /1.5/1.65	>13	13.4 /12.6/15.8 /9.4/9.85	0.10×0.17
[15]	5	1.8/ /2.5/3.3 /3.8/4.5	0.7 /0.28/0.8 /0.6/0.9	>8.5	11 /15/5 /5/5	0.32×0.19
[16]	5	1.8/ 3.5/4.5 /5.8/6.8	0.7 /0.28/0.8 /0.6/0.9	>15	4.8 /12/1.5 /4.5/0.59	0.18×0.15
[17]	5	0.6/ 0.9/1.2 /1.5/1.8	2.8 /2.9/2.9 /2.6/2.3	>13	5.8 /5.2/5.8 /8.2/8	0.52×0.05
[18]	5	2.1/ 3/4 /4.7/7.2	0.98 /1.78/1.22 /1.77/2.39	>14	N/A	0.16×0.07
[19]	5	1.5/ 2.5/3.5 /4.5/5.8	1.5 /1.8/0.9 /1.2/2.5	>11	4.5 /4.5/3.6 /4.5/2.7	0.24×0.17
[20]	5	0.94/ 2.42/3.7 /4.6/5.75	0.12 /0.68/0.28 /0.65/0.57	>15	110.6 /33.5/17.6 /16/20	0.24×0.17
This Paper	5	1.06/ 3.24/5.36 /8.55/10.78	0.35 /0.37/0.17 /0.19/0.20	>11	25.59 /22.22/19.48 /16.03/17.17	0.23×0.14

IV. CONCLUSION

This paper presents a novel compact pentaband bandpass filter using a dual path stub loaded step impedance resonator (SLSIR). This filter is fabricated on a single layer Roger Duroid RT/5880 substrate. The design filter achieves a compact size, good selectivity, low insertion loss, wide out of band rejection and simple design procedure and topology.

This compact pentaband bandpass filter is deemed suited for multiband applications in wireless communication systems.

REFERENCES

[1] R. Zhang and L. Zhu, "Design of a compact dual-band bandpass filter using coupled stepped-impedance resonators," *IEEE Microw. Wireless Compon. Lett.*, vol. 24, no. 3, pp. 155–157, Mar. 2014.
[2] M.-H. Weng, S.-W. Lan, S.-J. Chang, and R.-Y. Yang, "Design of dual-band bandpass filter with simultaneous narrow- and wide-bandwidth and a wide stopband," *IEEE Access*, vol. 7, pp. 147694–147703, 2019.
[3] Y. Feng, X. Guo, B. Cao, B. Wei, X. Zhang, F. Song, X. Lu, and Z. Xu, "Tri-band superconducting bandpass filter with controllable passband specifications," *Electron. Lett.*, vol. 50, no. 20, pp. 1456–1457, Sep. 2014.
[4] M. AbdulRehman and S. Khalid, "Design of tri-band bandpass filter using symmetrical open stub loaded step impedance resonator," *Electron. Lett.*, vol. 54, no. 19, pp. 1126–1128, Sep. 2018.
[5] S. Majidifar and M. Hayati, "New approach to design a compact triband bandpass filter using a multilayer structure," *TURKISH J. Electr. Eng. Comput. Sci.*, vol. 25, no. 5, pp. 4006–4012, 2017.
[6] X. M. Lin and Q. X. Chu, "Design of triple-band bandpass filter using TRN-section stepped-impedance resonators," in *Proc. Int. Conf. Microw. Millim. Wave Technol.*, Apr. 2007.
[7] Q.-X. Chu and X.-M. Lin, "Advanced triple-band bandpass filter using tri-section SIR," *Electron. Lett.*, vol. 44, no. 4, pp. 295–296, Feb. 2008.
[8] J.-Y. Wu and W.-H. Tu, "Design of quad-band bandpass filter with multiple transmission zeros," *Electron. Lett.*, vol. 47, no. 8, pp. 502–503, Apr. 2011.
[9] C.-M. Cheng and C.-F. Yang, "Develop quad-band (1.57/2.45/3.5/5.2 GHz) bandpass filters on the ceramic substrate," *IEEE Microw. Wireless Compon. Lett.*, vol. 20, no. 5, pp. 268–270, May 2010.
[10] J. Xu, "Compact high isolation quad-band bandpass filter using quad-mode resonator," *Electron. Lett.*, vol. 48, no. 1, pp. 28–30, 2012.
[11] L.-Y. Ren, "Quad-band bandpass filter based on dual-plane microstrip/DGS slot structure," *Electron. Lett.*, vol. 46, no. 10, pp. 691–692, 2010.
[12] H.-W. Wu and R.-Y. Yang, "A new quad-band bandpass filter using asymmetric stepped impedance resonators," *IEEE Microw. Wireless Compon. Lett.*, vol. 21, no. 4, pp. 203–205, 2011.
[13] S.-C. Lin, "Microstrip dual/quad-band filters with coupled lines and quasi-lumped impedance inverters based on parallel-path transmission," *IEEE Trans. Microw. Theory Tech.*, vol. 59, no. 8, pp. 1937–1946, May 2011.
[14] P. Ramanujam, K. Ramanujam, and M. Ponnusamy, "A novel asymmetrical interdigital coupled line-based penta-band bandpass filter design with enhanced selectivity employing square complementary split ring resonator," *Int. J. RF Microw. Comput.-Aided Eng.*, vol. 31, no. 12, Dec. 2021, Art. no. e22888.
[15] Y.-W. Chen, H.-W. Wu, Y.-W. Chen, R. Liu, H. Ye, and S.-K. Liu, "Design of new compact multi-layer quint-band bandpass filter," *IEEE Access*, vol. 9, pp. 139438–139445, 2021.
[16] L. Wang, S. Yang, L. Zhang, and B. Li, "Design of a compact quint-band bandpass filter using a symmetric dual-mode λ/4 resonator and a pair of inverted F-shaped resonators," *J. Electromagn. Waves Appl.*, vol. 36, no. 16, pp. 2289–2304, Nov. 2022.
[17] C. F. Chen, "Design of a compact microstrip quint-band filter based on the tri-mode stub-loaded stepped-impedance resonators," *IEEE Microw. Wireless Compon. Lett.*, vol. 22, no. 7, pp. 357–359, Jul. 2012.
[18] J. Ai, Y. Zhang, K. D. Xu, D. Li, and Y. Fan, "Miniaturized quint-band bandpass filter based on multi-mode resonator and λ/4 resonators with mixed electric and magnetic coupling," *IEEE Microw. Wireless Compon. Lett.*, vol. 26, no. 5, pp. 343–345, May 2016.
[19] K.-W. Hsu, W.-C. Hung, and W.-H. Tu, "Compact quint-band microstrip bandpass filter using double-layered substrate," in *IEEE MTT-S Int. Microw. Symp. Dig.*, Jun. 2013, pp. 1–4.
[20] Q. Yang, Y.-C. Jiao, and Z. Zhang, "Compact multiband bandpass filter using low-pass filter combined with open stub-loaded shorted stub," *IEEE Trans. Microw. Theory Techn.*, vol. 66, no. 4, pp. 1926–1938, Apr. 2018.
[21] I. Hunter, *Theory and Design of Microwave Filters*, no. 48. London, U.K.: IET, 2001.
[22] D. M. Pozar, *Microwave Engineering*. Hoboken, NJ, USA: Wiley, 2011.
[23] M. Makimoto and S. Yamashita, *Microwave Resonators and Filters for Wireless Communication: Theory, Design, and Application*, vol. 4. Cham, Switzerland: Springer, 2013.

BILAL MUSHTAQ received the B.S. and M.S. degrees in electrical engineering from HITEC University, Taxila, Pakistan, in 2011 and 2016, respectively. He is currently pursuing the Ph.D. degree with Riphah International University, Islamabad, Pakistan.

From 2012 to 2020, he worked as a Lecturer at the Electrical Engineering Department, Foundation University Rawalpindi Campus, Rawalpindi, Pakistan. He has been with Riphah International University, since 2021. His research interests include the design and synthesis of microwave filters, secure communication, and renewable energy.

SOHAIL KHALID (Member, IEEE) received the B.Eng. degree (Hons.) from CIIT Islamabad, in 2008, the M.Sc. degree in wireless networks from the Queen Mary University of London, in 2009, and the Ph.D. degree from Universiti Teknologi PETRONAS, Malaysia, in 2014. He is currently serving as an Associate Professor and the Head of Electrical Engineering Department with the Riphah International University, Islamabad, Pakistan, where he is teaching various bachelor's and master's engineering courses. His research interests include synthesis and design of passive microwave devices, millimeter wave applications for biomedical engineering, and biomedical signal processing.

MUHAMMAD ABDUL REHMAN received the bachelor's and M.Sc. degrees in computer sciences and telecom systems from Bahauddin Zakariya University, Multan, Pakistan, and the M.S. degree in electrical engineering from Riphah International University, Islamabad, Pakistan, where he is currently pursuing the Ph.D. degree in electrical engineering. He is also working as a Demonstrator with Riphah International University. His current research interest includes RF and microwave passive devices.